Incorporation of Metal Nanoparticles into Block Copolymer Nanodomains via in-Situ Reduction of Metal Ions in Microdomain Space

Takeji Hashimoto,*,†,‡ Masafumi Harada,†,§ and Naoki Sakamoto†,⊥

Hashimoto Polymer Phasing Project, ERATO, Japan Science and Technology Corporation, and Department of Polymer Chemistry, Graduate School of Engineering, Kyoto University, Kyoto 606-8501, Japan

Received March 12, 1999

Revised Manuscript Received July 19, 1999

In this communication we report the in-situ creation of metal nanoparticles in the microdomain space formed in block copolymers. The method involves reduction of palladium metal ions [Pd(II)] in a microdomain space formed in a concentrated solution of polyisoprene-*block*-poly(2-vinylpyridine) (PI-*b*-P2VP) in benzyl alcohol containing Pd(II) at 140 °C for 8 h. During the reduction process, benzyl alcohol acting as both a reduction agent for Pd(II) and a solvent for PI-*b*-P2VP is evaporated to result in a thin film. Before the reduction, Pd(II) will be shown to be uniformly distributed in the microdomain space. However, after the reduction, the Pd atoms are aggregated into nanoparticles and are selectively incorporated in microdomains comprised of poly(2-vinylpyridine) block chains (P2VP).

It is well established that block copolymers form various ordered nanodomain structures, whose morphology and characteristic length scale can be "tailored" by their molecular weight and composition.[1−3] Orientation of the ordered nanodomains can be also controlled by imposing applied fields such as shear,[4] electric field,[5] moving temperature gradient,[6] etc. Thus, we may come to a stage to explore principles and methods for "*nanoprocessing*" of block copolymer systems based on these nanodomains with an aim of developing some useful devices. For example, we can think of creating holes ("nanochannels") by using one of the nanodomains (such as cylinders, gyroid networks, etc.) in the matrix of others and plating of the surfaces of the nanochannels with metals.[7] We can also think of incorporating organic, inorganic, or metalic nanoparticles[8−13] in the microdomain space to create a "nanohybrid".

As for the selective inclusion of metal nanoparticles, there may be at least two ways. One involves first preparations of stabilized metal nanoparticles, and the stabilized particles are then incorporated or included in one of the nanodomains in block copolymers.[8−10] Another involves a reduction of the metal ions in one of the nanodomains.[11−13] In this work we will report our studies along the latter method.

Now among various reports along the latter method, the method employed by Schrock and co-workers[11] requires the synthesis of special block copolymers. The method employed by Ishizu and co-workers[12] does not require it, which may be an advantage of their method. However, this method by Ishizu and co-workers involves a number of steps such as a film formation, cross-linking of the films, quarternization and swelling of the cross-linked films with solvents, inclusions of metal ions into the quarternized and swollen films, reduction of the metal ions, and evaporation of solvents. In contrast, our method to be presented here is essentially one step: a reduction of concentrated polymer solutions containing Pd(II) at an elevated temperature (e.g., 140 °C) to obtain a film specimen in which metal nanoparticles are selectively included in one of the nanodomains. The new method is based on the experimental finding that ordered microdomains are formed above critical concentrations of block copolymers.[14−18]

PI-*b*-P2VP used in this work was synthesized as detailed elsewhere.[7,10] The PI block has a number-average molecular weight, M_n, of 1.8×10^4, and the P2VP block has $M_n = 1.26 \times 10^4$. The heterogeneity index of the block copolymer, M_w/M_n, is 1.04.

Nanodomain structures formed in the concentrated solutions or in the solid films were characterized by a small-angle X-ray scattering apparatus consisting of a 18 kW rotating-anode X-ray generator (M18XHF-SRA, MAC Science Co. Ltd., Yokohama, Japan), a graphite monochromator, a collimator, and a vacuum chamber for the incident-beam path and scattered-beam path and a position-sensitive detector. The SAXS profiles measured were corrected for absorption of X-ray beam, air scattering, and smearing effects.[19] The morphology of the thin films were investigated by a transmission electron microscope (TEM) (JEM-2000FXZ, JEOL, Tokyo, Japan) operated at 200 kV on the ultrathin sections obtained with a Reichert-Nissei Ultracut-S ultramicrotome. The sections were either unstained or stained with OsO_4 vapor or 1,4-diiodobutane.

A concentrated solution of PI-*b*-P2VP containing Pd(II) was first prepared using benzyl alcohol as a solvent and a reduction agent. For this purpose we dissolved a prescribed amount of PI-*b*-P2VP, benzyl alcohol, and Pd(acac)$_2$ into an excess amount of chloroform to obtain a dilute homogeneous block copolymer solution. After completely evaporating chloroform at room temperature, we measured again the weight of the solution to estimate the concentration of PI-*b*-P2VP.[20] The concentrated solution thus obtained was a clear brown solution without any reduction of Pd(II). The solution thus obtained was then subjected to the reduction of Pd(II)[21] at 140 °C, which simultaneously evaporated benzyl alcohol and resulted in formation of a dark thin film.

In this communication, we will present SAXS results for the following two solutions, designated system 1s and system 2s. System 1s is comprised of PI-*b*-P2VP/Pd(acac)$_2$/benzyl alcohol with a composition of the respective components given by 29.3/12.2/58.5 (wt %) ($w_{bcp} = 0.334$ and $w_{Pd(II)} = 0.293$). The weight fractions w_{bcp} and $w_{Pd(II)}$ will be defined later. System 2s is a solution corresponding to system 1s but free from Pd(acac)$_2$: PI-*b*-P2VP/benzyl alcohol ($w_{bcp} = 0.334$). We will present SAXS results for the corresponding two films

* To whom all correspondence should be addressed at Kyoto University.

† Japan Science and Technology Corporation.

‡ Kyoto University.

§ Present address: Department of Textile and Apparel Science, Faculty of Human Life and Environment, Nara Women's University, Nara 630-8506, Japan.

⊥ Present address: Asahi Chemical Industry Co., Ltd., Computer Science Department, 2-1, Samejima, Fuji, Shizuoka 416-8501, Japan.

10.1021/ma990378l CCC: $18.00
Published on Web 09/11/1999

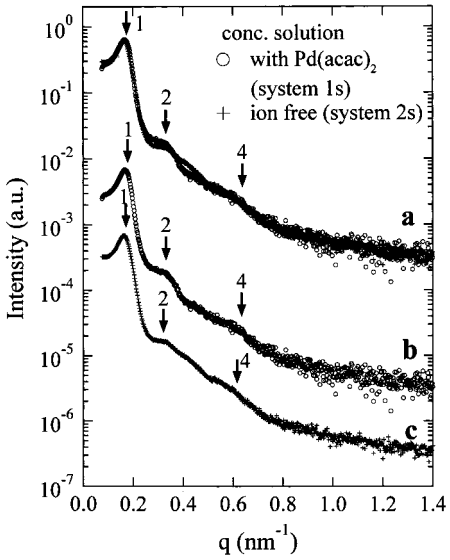

Figure 1. SAXS profiles from system 1s (PI-*b*-P2VP/Pd(acac)$_2$/benzyl alcohol = 29.3/12.2/58.5 (wt %) (w_{bcp} = 0.334 and $w_{Pd(II)}$ = 0.293)) and system 2s (PI-*b*-P2VP/benzyl alcohol = 33.4/66.6 wt %). Part a compares the two systems with and without Pd(acac)$_2$, while parts b and c show each system separately by shifting one of the two profiles vertically by 1 decade to avoid an overlap of the two profiles. The profile shown with + markers in part a and that in part c represent the profile from the solution free from Pd(acac)$_2$, while the profile shown with open circles in part a and that in part b represent the profile from the solution containing Pd(acac)$_2$ by 29.3 wt %. Here the s after 1s and 2s refers to the solution.

as well, designated system 1f and system 2f, obtained after the solvent evaporation at room temperature for about 1 week without any reduction of Pd(II). System 1f, PI-*b*-P2VP/Pd(acac)$_2$ ($w_{Pd(II)}$ = 0.293), was obtained after the solvent evaporation of system 1s. System 2f, PI-*b*-P2VP, was obtained after the solvent evaporation of system 2s. We shall present TEM results as well for the film specimens obtained after the reduction of the solution (denoted hereafter system 3s) having a composition of PI-*b*-P2VP/Pd(acac)$_2$/benzyl alcohol being 32.5/2.6/64.9 (wt %) (w_{bcp} = 0.334 and $w_{Pd(II)}$ = 0.074). Here w_{bcp} and $w_{Pd(II)}$ are defined w_{bcp} = (weight of PI-*b*-P2VP)/[(weight of PI-*b*-P2VP) + (weight of benzyl alcohol)] and $w_{Pd(II)}$ = (weight of Pd(acac)$_2$)/[(weight of Pd(acac)$_2$) + (weight of PI-*b*-P2VP)], respectively, which are the fraction of PI-*b*-P2VP relative to the solvent and that of Pd(II) relative to PI-*b*-P2VP, respectively, in either the ternary or the corresponding binary systems. Note that system 3s has a smaller value of $w_{Pd(II)}$ than system 1s. The system with a smaller fraction of Pd(II) was chosen for TEM observation, simply because a localization of Pd nanoparticles in the P2VP microdomains can be more clearly seen for the system with a small fraction of Pd(II) than for the system with a large fraction of Pd(II), as will be detailed elsewhere.[22]

Figure 1 shows typical SAXS profiles plotted on a semilogarithmic scale for system 1s (the profile shown with open circles in part a and the profile in part b) and for system 2s (the profile shown with + markers in part a and the profile in part c). The two profiles in parts b and c showed a multiple-order scattering maxima at q_m, $2q_m$, and $4q_m$ where q_m is magnitude of the scattering vector q [$q = (4\pi/\lambda)\sin(\theta/2)$] at the first-order scattering maximum.[23] Here λ and θ are wavelength of the incident X-ray beam (0.1542 nm) and scattering angle, respectively. Thus, the two concentrated solutions with and

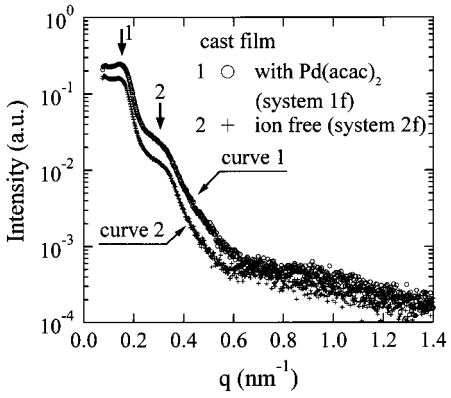

Figure 2. SAXS profiles from the film specimens cast from benzyl alcohol. Curve 1 shown with open circles represents the profile from system 1f (for the film containing Pd(acac)$_2$ by 29.3 wt % but without reduction), and curve 2 shown with + markers represents the profile from system 2f (for the film containing no Pd(acac)$_2$). Here the f after 1f and 2f refers to the film, and 1f denotes the film obtained from solution 1s.

without Pd(II) had the alternating lamellar microdomains rich in P2VP blocks and PI blocks. The two solutions have an almost identical repeat distance (37.6 and 39.0 nm for the solution with and without Pd(II), respectively). The two profiles in part a are seen to essentially overlap each other, revealing that they have almost identical alternating lamellar microdomain structures in terms of both the volume fractions of each phase and the electron density difference between the two phases. Since they have almost identical intensity, we can conclude that the Pd(acac)$_2$ are distributed equally well in the P2VP and PI lamellae.

The equal partition of the Pd(acac)$_2$ in both lamellae as inferred above may result from attractive interactions between ions and solvents being stronger than those between ions and polymers. This conjecture can be proven by comparing the SAXS profiles for systems 1f and 2f which were obtained respectively after a complete solvent evaporation from systems 1s and 2s. Figure 2 clearly shows that the ion containing dried film, i.e., system 1f (curve 1 drawn with open circles), has a stronger intensity than the ion free dried film, i.e., system 2f (curve 2 drawn with + markers), revealing that Pd(acac)$_2$ selectively coordinated in one of the nanodomains after the solvent evaporation, presumably in the P2VP phases (as will be proven later in Figure 4). This result implies that Pd(II)s have stronger attractions with the P2VP blocks than with the PI blocks in the absence of the solvent. The two film specimens show the profiles typical of the lamellar nanodomains with spacing of 44 nm, consistent with TEM observations shown later in Figure 3b,c.

Figure 3 shows the typical TEM images obtained after the reduction of system 3s (part a) together with those obtained for the following two reference systems: part b for the systems with Pd(acac)$_2$ but without the reduction (also obtained from system 3s) and part c for the neat block copolymer free from Pd(acac)$_2$ and Pd nanoparticles. In parts a and b the system contains Pd nanoparticles and Pd(acac)$_2$, respectively, by 7.4 wt %. In all the cases the systems show lamellar nanodomains (parts a−c). In part a Pd nanoparticles of diameter ca. 4 nm are more or less uniformly aligned along linear arrays, seemingly parallel to lamellar interfaces as expected from parts b and c, and the arrays of the Pd nanoparticles are arranged periodically with a spacing

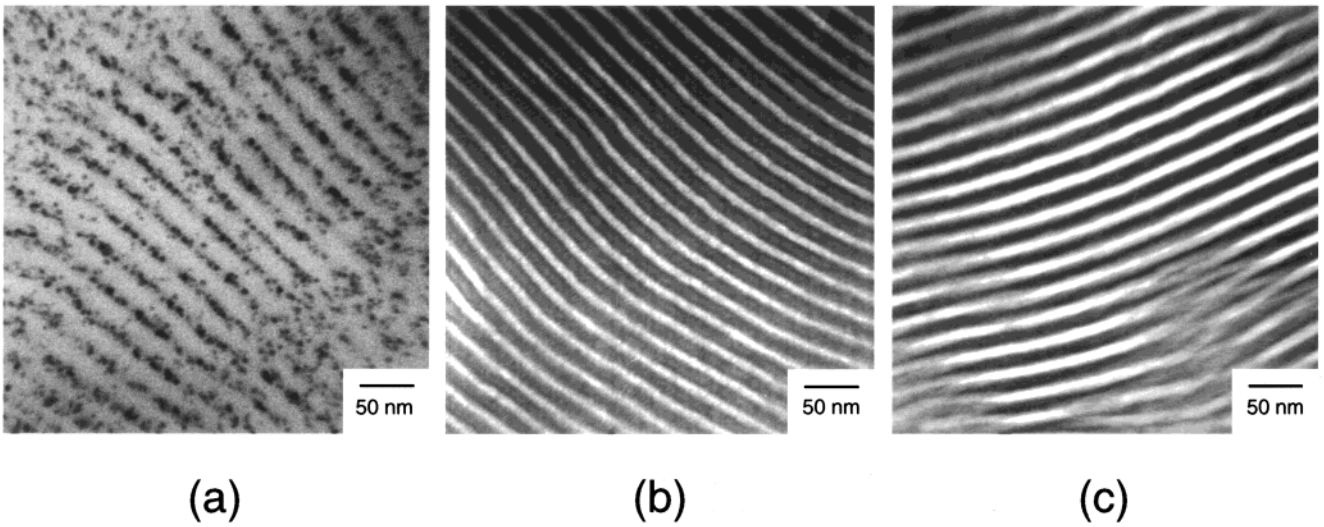

Figure 3. TEM images for the specimens obtained after the reduction of system 3s (PI-*b*-P2VP/$Pd(acac)_2$/benzyl alcohol = 32.5/2.6/64.9 (wt %) ($w_{bcp} = 0.334$ and $w_{Pd(II)} = 0.074$)) (a) for those obtained after solvent evaporation of system 3s without the reduction (b) and for the specimen free from $Pd(acac)_2$ (c). Images b and c were obtained with the ultrathin sections stained with OsO_4 vapor, while image a was obtained with unstained ultrathin sections. In image a, the dark dots are Pd nanoparticles which are aligned parallel to the interface between the P2VP lamellae and PI lamellae. In images b and c, the dark and bright phases are stained PI lamellae and unstained P2VP lamellae, respectively.

of ca. 30 nm.[24] The results shown in Figure 3 together with those in Figures 1 and 2 reveal the following two features in the particular conditions employed in this study: (1) The lamellar microdomains are maintained during the reduction and the solvent evaporation process.[25] (2) Pd(II) and the Pd nanoparticles incorporated in the P2VP phase do not perturb the lamellar microdomain structure (especially true for the case of $w_{Pd(II)} = 0.074$), though the concentration of Pd(II) in Figures 1 and 2 is different from that in Figure 3. In fact, the system containing $Pd(acac)_2$ by 29.3 wt % showed a morphology similar to Figure 3a except for a larger concentration of Pd nanoparticles after the reduction.[22]

Figure 4 shows the TEM images obtained on the film specimens after the reduction and further stained with OsO_4 (a) and 1,4-diiodobutane (b). Note that OsO_4 and 1,4-diiodobutane selectively stain the PI and P2VP phases, respectively. The results clearly reveal that the Pd nanoparticles are localized around the center of the P2VP phase. Before the reduction, Pd(II) ions are strongly solvated so that they are neutral to the PI and P2VP block chains and hence are distributed in both PI and P2VP lamellae with equal number densities, as pointed out earlier in this paper. However after the reduction, Pd atoms or clusters of Pd atoms will be coordinated only by P2VP block chains to result in localization around the center of P2VP lamellae. This point was clarified by an in-situ observation of SAXS profiles during the reduction process.[26] The distribution of metal ions in microdomain space before the reduction and the distribution of metal nanoparticles after the reduction depend generally on solvents and metals used in the system as well as working temperatures. The details about the morphology as a function of concentration of $Pd(acac)_2$, block copolymer compositions, reduction temperature, etc.,[22] as well as those about the in-situ analysis of the reduction process[26] will be reported elsewhere.

In summary we developed a new method of a selective incorporation of metal nanoparticles into block copolymer nanodomains by means of a one-step, in-situ, reduction of metal ions in ordered nanophases in concentrated block copolymer solutions.

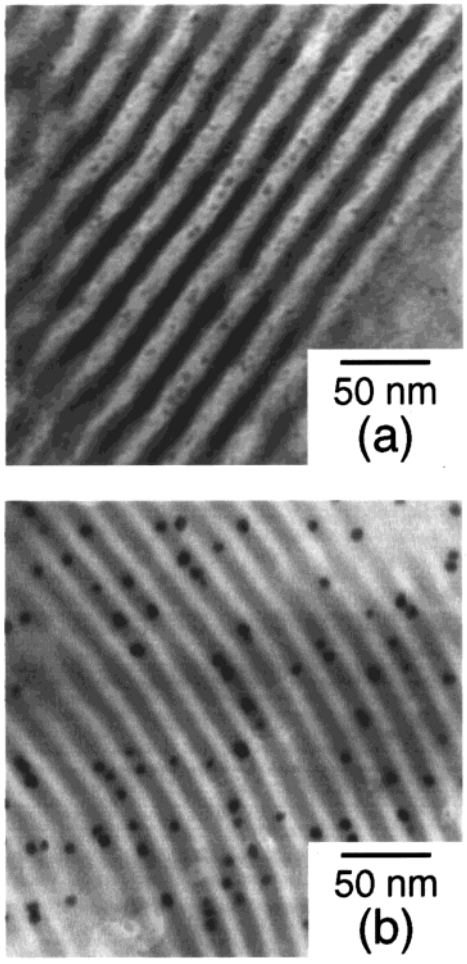

Figure 4. TEM images for the specimens obtained after the reduction of system 3s and further stained by OsO_4 vapor (a) and stained by 1,4-diiodobutane (b). In image a, the dark and bright phases are PI lamellae stained by OsO_4 and unstained P2VP lamellae, and dark dots are the Pd nanoparticles in P2VP phase. In image b, the dark and bright phases are P2VP lamellae stained by 1,4-diiodobutane and unstained PI lamellae, and the dark dots are Pd nanoparticles in P2VP lamellae.

Acknowledgment. The authors thank Y. Funaki, K. Tsutsumi, Y. Hirokawa, J. Yamanaka, and Y. Kanazawa, Hashimoto Polymer Phasing Project, for useful comments and technical support on this work.

References and Notes

(1) Inoue, T.; Soen, T.; Hashimoto, T.; Kawai, H. *J. Polym. Sci.* **1969**, *7*, 1283.
(2) Molau, G. E. In *Block Copolymers*; Aggarwal, S. L., Ed.; Plenum: New York, 1970.
(3) Matsuo, M.; Sagaye, S. In *Colloidal and Morphological Behavior of Block and Graft Copolymers*; Molau, G. E., Ed.; Plenum: New York, 1971; p 1.
(4) Keller, A.; Pedemonte, E.; Willmouth, F. M. *Nature* **1970**, *225*, 538.
(5) Amundson, K.; Helfand, E.; Davis, D. D.; Quan, X.; Patel, S. S.; Smith, S. D. *Macromolecules* **1991**, *24*, 6546.
(6) Hashimoto, T.; Bodycomb, J.; Funaki, Y.; Kimishima, K. *Macromolecules* **1999**, *32*, 952.
(7) Hashimoto, T.; Tsutsumi, K.; Funaki, Y. *Langmuir* **1997**, *13*, 6869 and references therein.
(8) Fogg, D. E.; Radzilowski, L. H.; Blanski, R.; Schrock, R. R.; Thomas, E. L. *Macromolecules* **1997**, *30*, 417.
(9) Zehner, R. W.; Lopes, W. A.; Morkved, T. L.; Jaeger, H.; Sita, L. R. *Langmuir* **1998**, *14*, 241.
(10) Tsutsumi, K.; Funaki, Y.; Hirokawa, Y.; Hashimoto, T. *Langmuir* **1999**, *15*, 5200.
(11) Ng Cheong Chan, Y.; Craig, G. S. W.; Schrock, R. R.; Cohen, R. E. *Chem. Mater.* **1992**, *4*, 885.
(12) (a) Saito, R.; Okamura, S.; Ishizu, K. *Polymer* **1992**, *33*, 1099. (b) Saito, R.; Okamura, S.; Ishizu, K. *Polymer* **1993**, *34*, 1183. (c) Saito, R.; Okamura, S.; Ishizu, K. *Polymer* **1993**, *34*, 1189. (d) Saito, R.; Ishizu, K. *Polymer* **1995**, *36*, 4119.
(13) Spatz, J. P.; Roescher, A.; Möller, M. *Adv. Mater.* **1996**, *8*, 337.
(14) Sadron, C.; Gallot, B. *Makromol. Chem.* **1973**, *164*, 301.
(15) Skoulios, A. In *Block and Graft Copolymers*; Burk, J. J., Weiss, V., Eds.; Syracuse University Press: Syracuse, NY, 1973.
(16) Hoffmann, M.; Kämpf, G.; Krömer, H.; Pampus, G. *Adv. Chem. Ser.* **1971**, *No. 99*, 351.
(17) Gallot, B. *Adv. Polym. Sci.* **1978**, *29*, 87.
(18) Hashimoto, T.; Shibayama, M.; Kawai, H. *Macromolecules* **1983**, *16*, 1093.
(19) Fujimura, M.; Hashimoto, T.; Kawai, H. *Mem. Fac. Eng., Kyoto Univ.* **1981**, *43*, 224.
(20) The boiling point and vapor pressure of chloroform are 61.8 °C and 200 mmHg at 25.6 °C, respectively, while benzyl alcohol has the boiling point of 204.7 °C and vapor pressure less than 1 mmHg at 25.6 °C and ca. 100 mmHg at 140 °C. Chloroform and benzyl alcohol are miscible in the temperature range used in this experiment.
(21) $Pd^{2+} + C_6H_5CH_2OH \rightarrow Pd + C_6H_5CHO + 2H^+$.
(22) Harada, M.; Hashimoto, T., manuscript in preparation.
(23) The suppression of the third-order peak at $3q_m$ is a consequence of one of the two phases (likely the PI phase) having a volume fraction close to $^1/_3$.
(24) Pd nanoparticles at top left and bottom right in Figure 3a appeared to be poorly aligned. This may be a perturbation effect induced by the sectioning process. Or they may look poorly aligned, though they are not actually so, due to the variation of lamellar orientation across different grains of lamellae.
(25) The generally morphology of ordered microdomains developed in solutions with or without Pd(II) and/or the Pd nanoparticles may vary with the concentration of PI-*b*-P2VP, simply because benzyl alcohol is not a neutral solvent for both block chains.
(26) Sakamoto, N.; Hashimoto, T., manuscript in preparation.

MA990378L